



This is a repository copy of *Characterisation of the temperature-dependent dark rate of Hamamatsu R7081-100 10" photomultiplier tubes.*

White Rose Research Online URL for this paper:

<https://eprints.whiterose.ac.uk/210935/>

Version: Submitted Version

---

**Preprint:**

Wilson, S.T. [orcid.org/0000-0002-6874-8600](https://orcid.org/0000-0002-6874-8600), Fargher, S., Foster, R.J. et al. (4 more authors) (Submitted: 2023) Characterisation of the temperature-dependent dark rate of Hamamatsu R7081-100 10" photomultiplier tubes. [Preprint - arXiv] (Submitted)

<https://doi.org/10.48550/arXiv.2306.10751>

---

© 2023 The Author(s). This preprint is made available under a Creative Commons Attribution 4.0 International License. (<https://creativecommons.org/licenses/by/4.0/>)

**Reuse**

This article is distributed under the terms of the Creative Commons Attribution (CC BY) licence. This licence allows you to distribute, remix, tweak, and build upon the work, even commercially, as long as you credit the authors for the original work. More information and the full terms of the licence here:

<https://creativecommons.org/licenses/>

**Takedown**

If you consider content in White Rose Research Online to be in breach of UK law, please notify us by emailing [eprints@whiterose.ac.uk](mailto:eprints@whiterose.ac.uk) including the URL of the record and the reason for the withdrawal request.



[eprints@whiterose.ac.uk](mailto:eprints@whiterose.ac.uk)  
<https://eprints.whiterose.ac.uk/>

# Characterisation of the Temperature-dependent Dark Rate of Hamamatsu R7081-100 10" Photomultiplier Tubes

---

S. T. Wilson,<sup>a,1</sup> S. Fargher,<sup>a</sup> R. Foster,<sup>a</sup> M. Malek,<sup>a</sup> M. Needham,<sup>b</sup> A. Scarff,<sup>a</sup> G. D. Smith,<sup>b</sup>

<sup>a</sup>*Department of Physics and Astronomy, University of Sheffield, Hounsfield Road, S3 7RH, UK*

<sup>b</sup>*School of Physics and Astronomy, University of Edinburgh, Mayfield Road, EH9 3JZ, UK*

*E-mail:* [stephen.wilson@sheffield.ac.uk](mailto:stephen.wilson@sheffield.ac.uk)

**ABSTRACT:** Dark noise is a dominant background in photomultiplier tubes (PMTs), which are commonly used in liquid-filled particle detectors for single-photon detection to see the results of particle interactions. A major contribution to dark noise is thermionic emission from the photocathode.

The dark noise of Hamamatsu R7081-100 PMTs is characterised in a temperature and purity controlled water tank, with the thermionic emission contribution isolated. The results suggest that the intrinsic dark rate of PMTs does not depend on the medium, but does follow Richardson's law of thermionic emission. There are external contributions to the overall observed PMT count rate identified, but the intrinsic PMT dark rate in water matches that measured in air.

**KEYWORDS:** Photon detectors for UV, visible and IR photons (vacuum) (photomultipliers, HPDs, others), Cherenkov detectors, Neutrino detectors

---

<sup>1</sup>Corresponding author.

---

## Contents

<b>1</b>	<b>Introduction</b>	<b>1</b>
<b>2</b>	<b>Experimental setup and measurements</b>	<b>2</b>
2.1	Photomultiplier tubes	2
2.2	Electronics	2
2.3	Water tank	2
2.4	Measurement procedure	2
<b>3</b>	<b>Analysis</b>	<b>4</b>
3.1	Pulse analysis	4
3.2	Thermionic emission	5
<b>4</b>	<b>Results</b>	<b>6</b>
<b>5</b>	<b>Discussion</b>	<b>8</b>
<b>6</b>	<b>Conclusion</b>	<b>9</b>

---

## 1 Introduction

Photomultiplier tubes (PMTs) are commonly used in particle detectors to detect photons resulting from particle interactions. In many detectors, particularly neutrino and dark matter detectors, the PMTs are submerged in a liquid medium such as pure water or liquid scintillator. However, they are typically characterised in air, normally at a single ambient temperature, before installation into a detector [1–7].

PMTs used for single-photon detection have characteristic single-photoelectron (SPE) pulses produced when a photon liberates an electron from the photocathode. However, photons are not the only mechanism by which electrons are liberated from the photocathode. Photons and other mechanisms are indistinguishable from the pulse, as they all cause electron emission making the pulses identical. A single electron will produce an SPE level pulse (a pulse with the same characteristics as a single-photon produced pulse).

Pulses produced in the absence of photons are referred to as “dark” pulses, PMTs each have a characteristic count rate of these, and are a dominant background to single-photon detection. Thermionic emission, where an electron is liberated from the photocathode by thermal energy, is one of the major mechanisms that produces dark counts and should be characterised in detail.

It has been seen in detectors that the rate of pulses changes depending on the medium the PMTs are installed in and its conditions, e.g. in the LUX-ZEPLIN dark matter detector [8]. As such, it is important to characterise PMTs in a realistic dielectric and magnetic environment, and with

varying temperature to understand the performance and thermionic dark noise contribution that can be expected in a detector. Here, the characterisation of the temperature-dependent dark noise of 10" Hamamatsu R7081-100 PMTs when submerged in pure water is presented.

## 2 Experimental setup and measurements

### 2.1 Photomultiplier tubes

The PMTs used in these tests are low radioactivity Hamamatsu R7081-100 10" diameter tubes with a waterproof potting applied. An 80 m BELDEN YR53485 cable, connected by the vendor, is used to supply positive high voltage (HV) and provide a return path for the signal as they are alternating current (AC) coupled. The electronics in the PMT base has an impedance of 50  $\Omega$ .

### 2.2 Electronics

The PMTs are powered via a CAEN V6534P positive polarity HV board. As the PMTs are AC coupled, the AC signal and direct current (DC) HV need to be separated. A custom "splitter" board, using a capacitor in a resistor-capacitor circuit as a high-pass filter, is used [9] to block the DC components and eliminate the DC offset from the AC signals. The splitter is designed to have the same impedance, 50  $\Omega$ , as the electronics in the PMT base to reduce signal reflections caused by impedance mismatches.

As the SPE signal from these PMTs has a mean amplitude of approximately 4 mV, the signal is amplified by a CAEN N979 10x fast amplifier. It is then digitised by a CAEN V1730B 500 MS/s digitizer where a 10 kHz external trigger is used to open a 220 ns acquisition window. The digitiser is read out via an optical link to a CAEN A2818 PCI CONET controller.

### 2.3 Water tank

To characterise the PMTs in water, they need to be completely submerged. To achieve this, a 2000 L (2 m x 1 m x 1 m) 316L stainless steel water tank has been constructed at the University of Sheffield. The water in the tank is purified by a Veolia system to 18.2 M $\Omega$ ·cm using a series of filters, a deionising cylinder and an ultraviolet lamp, and the temperature can be controlled in the 4 °C to 30 °C range by a heat exchange unit. The temperature of the water in the tank and purification system is measured by a series of temperature probes, and the resistivity of the water is measured as it enters and exits the purification system. The system is insulated, and the temperature is stable within 0.1 °C in all but extreme ambient conditions. The resistivity of the water remains consistent at approximately 12.5 M $\Omega$ ·cm in the tank during data taking periods.

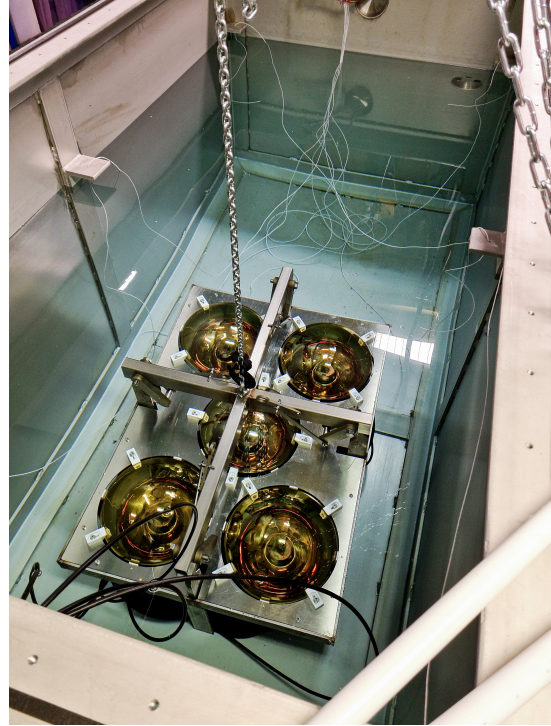
To ensure that no stray light enters the tank, and artificially increases the dark rate, the tank, and lid are covered by layers of black plastic sheets, and the feedthroughs used for PMT cables and monitoring of the conditions are also wrapped. [Figure 1a](#) shows the outside of the tank when it is set up for testing, with [Figure 1b](#) showing how the PMTs are lowered into the tank.

### 2.4 Measurement procedure

To take measurements, a set of up to 5 PMTs are placed in a holder and lowered into the tank. A lid is placed on the tank and the cables connected to the splitter board after passing through a safe high voltage (SHV) to SHV feedthrough.



(a) The 2000 L tank used to submerge PMTs in water.



(b) A batch of PMTs in the holder being lowered into the tank.

**Figure 1:** (a) The 2000 L tank used to submerge PMTs in pure water. The inside of the tank is optically isolated from its surroundings, and the water purity and temperature are controlled. (b) A batch of five PMTs inside the tank. Covers can be added to each PMT individually for further optical isolation.

To measure the rate of dark pulses, 15 minute runs with the 10 kHz external trigger are used. Each run equates to 1.98 s of live time, or approximately  $9 \times 10^6$  waveforms each 220 ns in length. Four runs are taken across a two hour period at each temperature to ensure consistency between runs. The water temperature is adjusted between 7 °C and 25 °C in 2.5 °C steps, except for between 12 °C and 15 °C where 0.5 °C steps are used. This region is chosen to surround the operating temperature of Super-Kamiokande [10].

As measurements of the dark rate are desired, the inside of the tank needs to be kept optically isolated from the tank's surroundings. To confirm no external light is entering the tank, runs are taken with the room lights on and off for each PMT deployment. The final data is taken with the room lights off.

When PMTs are exposed to significant levels of light, they have an increased dark rate for several hours to days after the exposure. This "cooldown" period is measured by exposing the PMTs to large levels of light and then recording the dark rate every hour for five days at a fixed temperature. The outcome, in Figure 2, shows that after approximately two and a half days the dark rate is at its pre-exposure level. Therefore, the PMTs are left in total darkness for at least two and a half days, 60 hours, before attempting to take measurements.

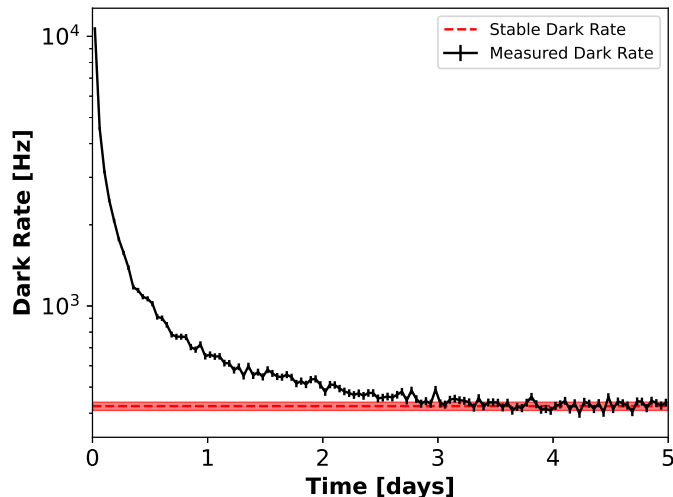


**Figure 2:** The dark rate with time in complete darkness after large light exposure for PMT0103 (black). The rate takes around two and a half days to settle at the pre-exposure level of 425 Hz (red, dashed) within error.

Despite light from outside the tank being blocked from entering the system, light can still be produced inside the tank. Cosmic ray muons will produce Cherenkov radiation as they pass through the water. As the tank is on the Earth’s surface and near sea level, the rate is approximately  $1 \text{ cm}^{-2} \text{ min}^{-1}$  [11]. This, alongside the large amount of light produced per muon and the amount the light reflects in the steel tank, produces a significant increase in SPE level pulses observed by the PMTs. Alongside muons, radioactive backgrounds, in particular from the PMT glass, can produce Cherenkov and gamma radiation. It is also possible for light to be produced by the final dynodes in the PMT itself [12]. Most single-photon detecting PMTs have countermeasures [13], but it is possible for photons to escape and trigger that or neighbouring PMTs.

To combat the light produced inside the system and isolate the thermionic emission and intrinsic dark rate, each PMT is individually covered in a black plastic sheet. This allows them to be optically isolated from each other and any light produced in the water.

### 3 Analysis

#### 3.1 Pulse analysis

An SPE pulse is characterised as having a mean amplitude of 40 mV after amplification, and a width of around 20 ns where the rise is very sharp (few ns) and the fall is exponential [9]. An example is shown in Figure 3. A threshold of 25% of the mean SPE amplitude, 10 mV in this case, is used in line with Hamamatsu [14], and a rise time cut of  $< 20 \text{ ns}$  is applied. An upper amplitude limit of 80 mV is applied to remove multiple-photon backgrounds e.g. from cosmological muons. The probability of multiple true dark pulses in a single acquisition window is assumed to be negligible.

Despite attempting to match the impedance between the PMT electronics and the splitter board, there is still a mismatch due to the circuit board used in the splitter board. This mismatch causes reflections of large pulses in the cables, which causes a large baseline shift within the data

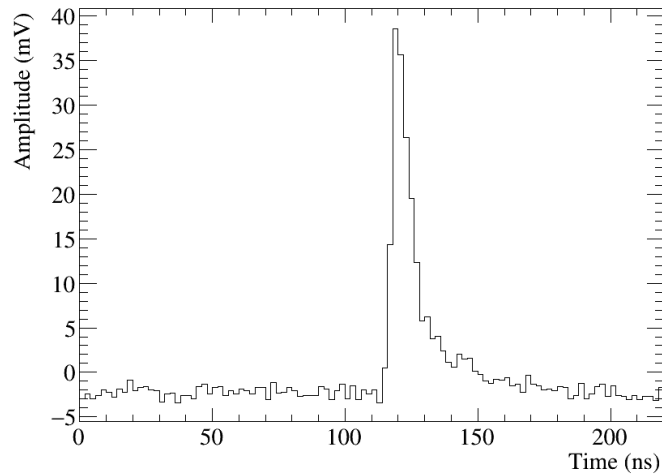


**Figure 3:** Typical SPE level pulse after 10x amplification. These make up approximately 90% of the pulses above threshold.

acquisition window when these pulses occur just before the external trigger. The system as a whole also contributes to these shifts. The water circulation systems contain several pumps and motors, and the water tank is difficult to shield. As such, the system is susceptible to noise which causes further shifts in the baseline. SPE level pulses can be impacted by these baseline shifts, as shown in [Figure 4](#).

To compensate for this, a baseline correction similar to the Linear Common Mode Suppression algorithm described in [15] is applied. This correction has several steps:

1. The mean of the waveform is subtracted.
2. Any linear slope in the data is corrected for.
3. Data points more than one standard deviation from the mean are removed.
4. The mean of the new waveform is subtracted.
5. Any linear slope in the new waveform is corrected for.
6. Outlying data points with corrections applied are re-added to the waveform.

This acts to counter the reflections and leave a pulse with a flat baseline centred on 0 mV such as the one in [Figure 4](#), making the analysis of SPE level pulses more robust.

### 3.2 Thermionic emission

Thermionic emission is modelled using Richardson's law [16] in [Equation 3.1](#),

$$N = AT^2 \exp\left(\frac{-e\phi}{k_B T}\right). \quad (3.1)$$

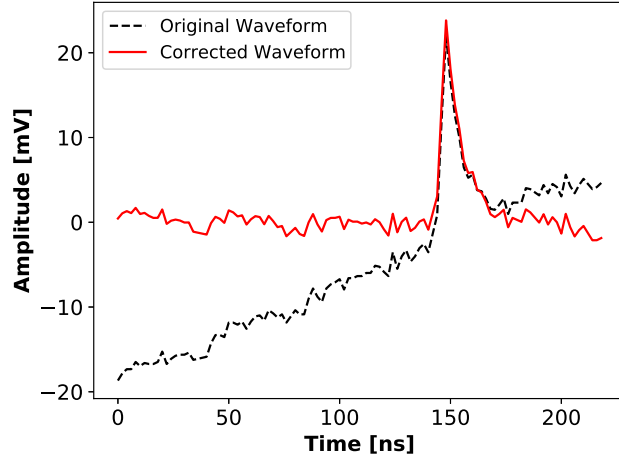


**Figure 4:** The corrections applied to a waveform with a shifted baseline (red, solid), with the original waveform (black, dashed) shown for reference.

Here,  $N$  is the rate of electrons emitted from the photocathode by thermionic emission,  $A$  is a scaling factor containing a material-specific correction factor,  $T$  is the absolute temperature,  $\phi$  is the work function,  $e$  is the electron charge and  $k_B$  is the Boltzmann constant. A constant offset is also applied.

The electrons emitted will produce SPE level pulses, at the rate  $N$ . By measuring the dependence of  $N$  on  $T$ , the work function  $\phi$  can be obtained for the photocathode and any divergence between the data and Richardson’s law for thermionic emission can be observed.

## 4 Results

The results shown in [Figure 5](#), show that Richardson’s law fits the data well. The data occasionally has a small plateau-effect below 15 °C as the thermionic emission component of dark rate reduces. Results for one batch of three covered PMTs are shown in [Figure 5a](#). A comparison between the SPE level pulse rates when covered and uncovered for these PMTs is shown in [Figure 5b](#), suggesting that when the PMTs are uncovered, more than half of the counts come from sources other than dark pulses.

The work functions for the PMTs, obtained by fitting Richardson’s law to the data, match the range measured in air [\[9\]](#) with values between 1.2 and 1.5 eV.

Runs with the room lights on and off are consistent with each other, confirming no stray light enters the system.

To confirm the results, a series of tests are conducted on PMT0103 in isolation. To do this, PMT0103 is deployed in the tank on its own. Temperature-dependent measurements of dark rates are taken and compared to the measurements taken from PMT0103 when deployed with other PMTs. The results, in [Figure 6](#), show very little difference between the two runs. The PMT is also exposed to light before measuring the dark rate every hour for five days which confirms the optical cooldown period of 60 hours is sufficient, with results in [Figure 2](#).

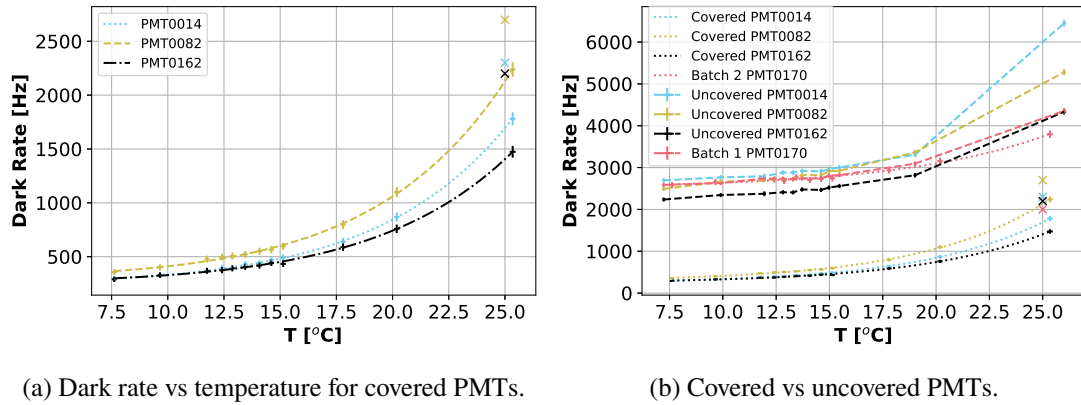


**Figure 5:** The SPE level pulse rate for a batch of PMTs. (a) shows the dark rate with the PMTs covered. (b) shows a comparison between the SPE level rates when the PMTs are optically isolated from their surroundings by a cover and those exposed to the whole system, with PMT0170 kept uncovered to act as a control. Covering the PMTs lowers the SPE level count rate significantly, and brings them closer to the measurements made by the vendor [14] (“x” at 25 °C). The measurements for the covered PMTs have the fit to Richardson’s law superimposed.

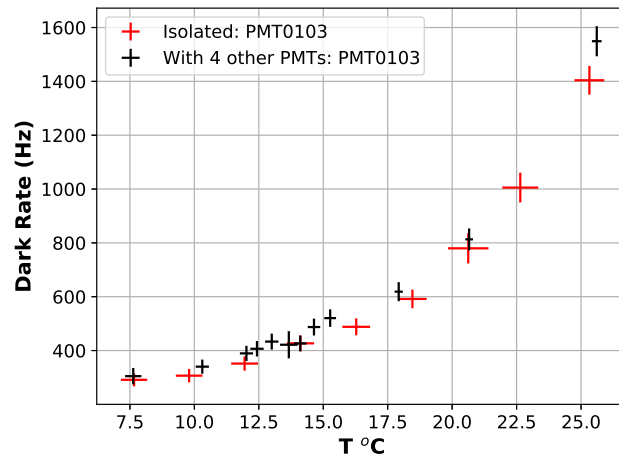


**Figure 6:** The dark rate with temperature for PMT0103 measured when the PMT is part of a batch of PMTs (black) compared to in isolation (red).

The impact of water resistivity is tested by bypassing the deionising cylinder and allowing the water resistivity to drop gradually, and taking data every hour during this. The water resistivity and dark rate results, in Figure 7, confirm the resistivity has no clear impact on the intrinsic PMT dark rate.

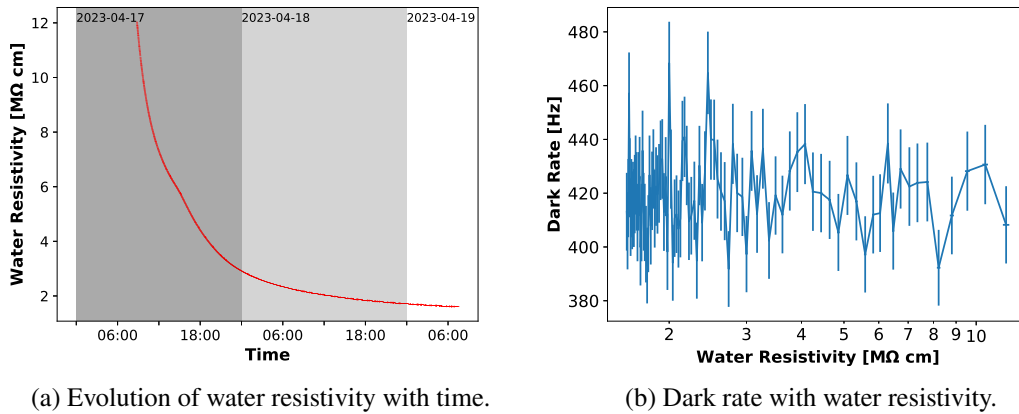


**Figure 7:** (a) The water resistivity with time after the deionising cylinder is bypassed. The resistivity drops when the deionising cylinder in the filtration system is bypassed. (b) The dark rate of a covered PMT with resistivity. There is no clear connection between intrinsic PMT dark rate and water resistivity.

## 5 Discussion

The results of the measurements of temperature-dependent dark rate across thirteen PMTs are in good agreement with thermionic emission as modelled using Richardson’s law in [Equation 3.1](#) in the 15 °C to 25 °C temperature range. However, below 15 °C there are occasionally small deviations above the expected rate as thermionic emission rates reduce. This suggests that there are non-thermionic emission contributions to the dark rate that become more dominant at lower temperatures. It is seen in [13, 17] that the temperature-dependent dark rate does not always follow Richardson’s law of thermionic emission.

An assay of the PMT glass, performed at the Boulby UnderGround Screening (BUGS) facility and shown in [Table 1](#), suggests that the PMT glass has a low contribution to the background at approximately  $3.4 \text{ Bq kg}^{-1}$ . The mass of these PMTs is 1.4 kg, yielding  $< 5 \text{ Bq}$  per PMT assuming the glass is the majority of the PMT mass. Not all of these events will cause light emission, further lowering the contribution to the overall dark rate.

Measurements of the SPE level pulse rate with changing water resistivity confirm that the water resistivity has negligible impact on the intrinsic SPE level pulse rate.

The largest non-thermal contribution to SPE level counts in a liquid medium is light. Despite the system being optically isolated from its environment, the liquid fill allows light production via particle interactions from cosmic ray particles and radioactive decays. Cosmic ray muons are incident on the tank at an expected rate of the order several hundred Hz as the tank has a  $2 \text{ m}^2$  top surface area, and a further  $6 \text{ m}^2$  on the sides. This light is also likely to be reflected, which will further increase the number of photons hitting PMTs, due to the steel tank. Without simulations, it is hard to quantify the expected number of hits from muon-produced photons, but it is expected to be a significant contributor to the total number of counts observed by the PMTs. Along with the direct detection of photons, the consistent light exposure leads to a prolonged increase in PMT activity

Isotope	mBq/kg	ppx
$^{238}\text{U}$	660(40)	54(3)
$^{226}\text{Ra}$	430(20)	35(1)
$^{210}\text{Pb}$	610(50)	50(4)
$^{235}\text{U}$	30(5)	50(7)
$^{228}\text{Ra}$	440(20)	108(5)
$^{224}\text{Ra}$	370(10)	89(2)
$^{40}\text{K}$	830(50)	27(2)

**Table 1:** PMT glass assay results from data taken at the BUGS facility using a Mirion (Canberra) BE6530 BEGe-type HPGe detector. Uncertainties in mBq/kg are  $1\sigma$  statistical errors only. True coincident summing effects are not accounted for, and introduce an additional error of up to  $O(10\%)$ . For comparison only, the  $^{235}\text{U}$  value is given as a  $^{238}\text{U}$  ppb equivalent where conversion is performed using the standard  $^{nat}\text{U}$  activity ratio for  $^{238}\text{U}$ :  $^{235}\text{U}$  of 21.6 [18].

leading to a further increase in the SPE level pulse rate. As such, simply vetoing cosmic ray muons and accounting for radioactive backgrounds might not allow all contributions to the SPE pulses due to light to be removed. Beyond light production in the tank, high gain PMTs are known to produce light in the final dynodes around the anode [12]. This light can trigger both the PMT emitting the light and its neighbours. By optically isolating PMTs from the system and their neighbours, the SPE level pulse rate drops by a factor of  $\sim 2.5$  as shown in Figure 5b.

A comparison between dark rate measurements made in water and air (both in [9] and by the vendor [14]) at  $25\text{ }^\circ\text{C}$  is presented in Table 2. The measurements in air show good agreement. The water measurements agree with expectation when the time in darkness before data taking is accounted for. The measurements made in air are after approximately 18 hours in complete darkness, whereas those in water are after at least 60 hours. The dark rate reduces significantly over this time. For PMT0103, the dark rate after 18 hours is 1.8 times the rate after 60 hours, as shown in Figure 2.

This is significant for detector application, as it suggests that there is no intrinsic difference in PMT dark rate when the medium of deployment changes. Therefore, any differences seen in PMT rates when in a liquid are likely to be due to external contributions such as light production in the system. In the case of LUX-ZEPLIN [8], the raised pulse rates that occur after the tank is opened and the water resistivity drops is likely related to contaminants in the water or optical cooldown after light exposure, and not an intrinsic effect of water resistivity on the PMTs.

## 6 Conclusion

The temperature-dependent dark rate of Hamamatsu R7081-100 10" PMTs has been characterised when submerged in water, and shows a good match to the measurements taken in air [9] and by the vendor [14]. Richardson's law of thermionic emission fits the data well, especially in the  $15\text{ }^\circ\text{C}$  to  $25\text{ }^\circ\text{C}$  range, with other contributions becoming more noticeable at lower temperatures.

The impact of light on the SPE level pulse rate is significant, and simply using a light tight water tank is not sufficient to remove all light. This is due to light production in water from cosmic

PMT ID	Dark Rate at 25 °C [Hz] (after time in dark)		
	Water (60 hours)	Air (18 hours)	Vendor
14	1,708	2,409	2,300
82	2,149	2,793	2,700
162	1,396	2,141	2,200
3	1,804	4,401	3,600
112	1,730	1,855	1,500
159	1,235	2,489	2,000
26	1,329	3,702	3,600
104	3,276	1,667	1,500
143	865	1,439	1,400
155	3,535	4,193	5,000
15	1,397	2,259	2,200
29	1,487	1,729	1,900
103	1,428	1,759	1,600
148	954	1,892	2,100

**Table 2:** The dark rate measured at 25 °C in water, air [9] and by the vendor (air) [14]. The tests in water were conducted after at least 60 hours in complete darkness, the other tests after approximately 18 hours. Uncertainties are 1 - 4% for the water and air measurements.

ray muons, radioactive backgrounds and possibly the PMTs themselves. The impact of radioactivity from individual PMTs and water resistivity are shown to have a negligible effect on the intrinsic dark rate, but exposure to light has a lasting impact. The source of raised SPE level pulse rates in liquid detectors is likely to be external to the PMTs.

It can be concluded that intrinsic PMT dark rate is consistent across different media, and that characterising a PMT in air is sufficient, based on the comparison of temperature-dependent dark rates measured in air and water when all light is removed.

## Acknowledgments

The authors would like to express our gratitude to Matt Thiesse at the University of Sheffield for his design and construction of the water tank used for this testing. We would also like to express our thanks for his regular review of the concepts and methods involved in this work.

The authors would also like to thank Paul Scovell and the team at the BUGS facility at STFC's Boulby Underground Laboratory for their assay of the PMT glass.

Finally, we would like to acknowledge the work done by Tom Shaw and Steve Quillin of the Atomic Weapons Establishment in the United Kingdom. Tom designed the first version of the electronics setup used, whilst Steve was involved in the early stages of the waveform analysis.

## References

- [1] Y. Zhang, Z. Wang, M. Li, Y. Zhang, Y. Wang, Z. Peng et al., *Study of 20-inch PMTs dark count generated large pulses*, *J. Instrum.* **17** (2022) P10048.
- [2] T. Kaptanoglu, *Characterization of the Hamamatsu 8" R5912-MOD Photomultiplier tube*, *Nucl. Instrum. Methods Phys. Res. A: Accel. Spectrom. Detect. Assoc. Equip.* **889** (2018) 69.
- [3] B. Herold and O. Kalekin, *PMT characterisation for the KM3NeT project*, *Nucl. Instrum. Methods Phys. Res. A: Accel. Spectrom. Detect. Assoc. Equip.* **626-627** (2011) S151.
- [4] J. Brack, B. Delgado, J. Dhooghe, J. Felde, B. Gookin, S. Grullon et al., *Characterization of the Hamamatsu R11780 12 in. photomultiplier tube*, *Nucl. Instrum. Methods Phys. Res. A: Accel. Spectrom. Detect. Assoc. Equip.* **712** (2013) 162.
- [5] J. Aguilar, A. Albert, F. Ameli, P. Amram, M. Anghinolfi, G. Anton et al., *Study of large hemispherical photomultiplier tubes for the ANTARES neutrino telescope*, *Nucl. Instrum. Methods Phys. Res. A: Accel. Spectrom. Detect. Assoc. Equip.* **555** (2005) 132.
- [6] C. Bauer, E. Borger, R. Hofacker, K. Jänner, F. Kaether, C. Langbrandtner et al., *Qualification tests of 474 photomultiplier tubes for the inner detector of the Double Chooz experiment*, *J. Instrum.* **6** (2011) P06008.
- [7] R. Abbasi, Y. Abdou, T. Abu-Zayyad, J. Adams, J. Aguilar, M. Ahlers et al., *Calibration and characterization of the IceCube photomultiplier tube*, *Nucl. Instrum. Methods Phys. Res. A: Accel. Spectrom. Detect. Assoc. Equip.* **618** (2010) 139.
- [8] C. Wright, "Monitoring Tools for the LUX-ZEPLIN Outer Detector." IoP Joint APP and HEPP Annual Conference, 2023.
- [9] O. Akindede, A. Bernstein, S. Boyd, J. Burns, M. Calle, J. Coleman et al., *Acceptance tests of Hamamatsu R7081 photomultiplier tubes*, *J. Instrum.* **18** (2023) P08015.
- [10] K. Abe, Y. Hayato, T. Iida, K. Iyogi, J. Kameda, Y. Kishimoto et al., *Calibration of the Super-Kamiokande detector*, *Nucl. Instrum. Methods Phys. Res. A: Accel. Spectrom. Detect. Assoc. Equip.* **737** (2014) 253.
- [11] H. Gadey, S. Chatzidakis and A.T. Farsoni, *Monte Carlo characterization of the cosmic ray muon flux in shallow subsurface geological repositories intended for disposal of radioactive materials*, *Appl. Radiat. Isot.* **163** (2020) 109209.
- [12] H.R. Krall, *Extraneous light emission from photomultipliers*, *IEEE Trans. Nucl. Sci.* **14** (1967) 455.
- [13] A.G. Wright, *The Photomultiplier Handbook*, Oxford University Press (June 2017).
- [14] Hamamatsu, *Water-proof Type Photomultiplier Assembly R7081-100-10-WA-S80: Tentative Data Sheet*, December 2017.
- [15] G. Haefeli, *Contribution to the development of the acquisition electronics for the LHCb experiment*, Ph.D. thesis, Ecole Polytechnique, Lausanne, 2004.
- [16] O.W. Richardson, *Electron Emission from Metals as a Function of Temperature*, *Phys. Rev.* **23** (1924) 153.
- [17] P.B. Coates, *Thermionic emission from photocathodes*, *J. Phys. D: Appl. Phys* **5** (1972) 1489.
- [18] International Atomic Energy Agency (IAEA), "Depleted Uranium." <https://www.iaea.org/topics/spent-fuel-management/depleted-uranium>, accessed 19th May 2023.